Research Article | Vol. 28, No. 3 / 3 February 2020 / Optics Express 2818
Optics EXPRESS

Optical-field topological phase transition in nonlinear frequency conversion

WANG ZHANG,[1] JIE TANG,[1] YANG MING,[1,2] CHAO ZHANG,[1,3] AND YANQING LU[1,4]

[1]National Laboratory of Solid State Microstructures, College of Engineering and Applied Sciences, Nanjing University, Nanjing 210093, China
[2]School of Physics and Electronic Engineering, Changshu Institute of Technology, Suzhou 215000, China
[3]zhch@nju.edu.cn
[4]yqlu@nju.edu.cn

Abstract: The topological effects accompanied by phase structuring during the interaction between optical fields and nonlinear crystals are presented and demonstrated. The topological phase transition in the optical field is determined during the quasi-phase matched second harmonic frequency conversion process. The mapping relationship between the corresponding topological invariant and the phase parameters is derived, and two critical transition points are obtained. The transition of the total orbital angular momentum (OAM) in the propagation direction is verified to be the physical origin of this topological regulation through OAM spectrum analysis. This work provides a new perspective for examining nonlinear light-matter interaction, which can inspire promising applications in structured light generation and optical information processing.

1. Introduction

The optical field, comprising electromagnetic waves that oscillate in time and propagate in space, is often described by the frequency, polarization, wave-vector, and phase. The shaping of light in these degrees of freedom, and in the spatial and time domain has always been a hotspot in the field of optics [1]. Many studies have been performed using reconfigurable liquid crystals [2–4] and structured metasurfaces [5,6] with dynamic, geometric [7,8] or resonance phase [9,10] control. In the past few years, topology, which is the mathematical concept concerning the conserved properties under continuous deformation, has been applied as a new indispensable degree of freedom to describe physical systems. Characterizing the quantized global behaviors of both classical and quantum wave functions, topology paves a way for the discovery of new phases of matter [11,12] with unprecedented applications [13]. In the area of photonics, considerable attention has been paid to material systems, focusing on the topological features defined with respect to the dispersion bands in reciprocal space, and remarkable advances have been made [13–15]. In addition, of late, the topology of the structured optical field itself defined with respect to the phase in transverse space [16], and the topological effects during light-matter interaction, in particular, are attracting increasing attention.

Nonlinear processes in which waves are mixed through the nonlinear component of the induced material polarization provide abundant possibilities for optical field regulation through nonlinear susceptibility engineering. With electric field poling [17], which is a mature fabrication method, quadratic nonlinear susceptibility can be arbitrarily modulated two-dimensionally, while the linear susceptibility remains constant [18–20]. Combining the new technology of femtosecond laser writing, nonlinear susceptibility modulation can even be extended to three dimensions [21,22]. Over the past decades, in this area, it has been extensively investigated using technologies such as computer-generated holography [23] and nonlinear volume holography [24]; for example, the nonlinear generation of Airy beams [25], two-dimensional nonlinear optical imaging [26], and the all-optical Stern-Gerlach effect [27]. To date, the spatial and spectral responses of the optical

#382818 https://doi.org/10.1364/OE.382818
Journal © 2020 Received 8 Nov 2019; revised 2 Jan 2020; accepted 6 Jan 2020; published 21 Jan 2020

Optics EXPRESS

field during nonlinear frequency conversion have been extensively studied and well determined; however, the modulation effects on the topology of the optical field remain unknown.

In this work, we demonstrate that the optical field topology can be directly modulated using nonlinear photonic crystals: the topological phase transition is accompanied by frequency conversion under certain situations. We study various phase-structured optical fields with different topologies during the nonlinear process of second harmonic frequency generation (SHG), and quantify the mapping relationships between the phase parameters and topological invariants. In particular, we calculate and analyze the orbital angular momentum (OAM) spectrum to reveal the inner mechanism and physical connotation of this topological modulation. This sheds new light on spatial optical applications and photonic information processing.

2. Phase structuring in nonlinear frequency conversion

As the optical field topology is directly related to the transverse spatial distribution of the phase, we first examine the phase evolution during nonlinear frequency conversion. As an example, we investigate the nonlinear second harmonic frequency conversion process through various pump optical fields with different phase distributions as shown in Fig. 1.

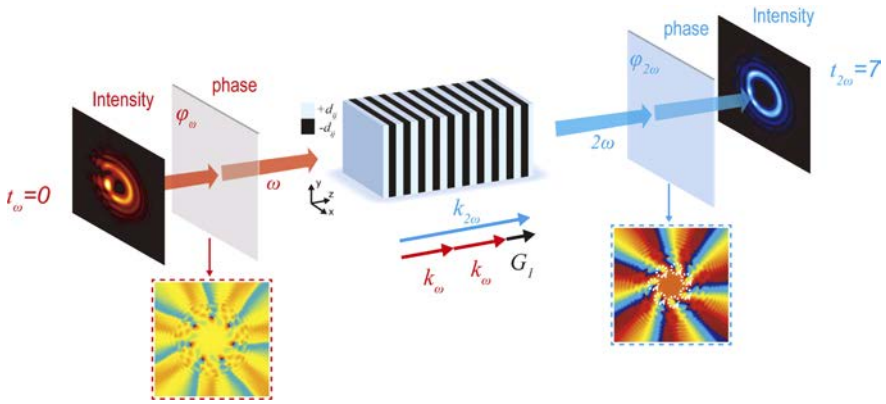

Fig. 1. Schematic illustration of the topological phase transition of the optical field during nonlinear frequency conversion. As an example, a pump optical field with a topological invariant $t_\omega = 0$ is converted into an SH optical field with a topological invariant $t_{2\omega} = 7$after the quasi-phase matched SHG process. The wave-vector matching is indicated in the center of the illustration.

When light is incident on nonlinear materials, for example $LiNbO_3$, polarization (dipole moment per unit volume) is induced within the materials. In addition to the linear polarization associated with the dispersion and absorption of the material, nonlinear polarization acts as a light generation source at new frequencies. In the nonlinear SHG process, the first nonlinear term, quadratic nonlinearity $d_{il}E^2$, is applied for the interaction of two pumping waves with the same frequency $\omega_1 = \omega$ and a second harmonic (SH) wave with frequency $\omega_2 = 2\omega$. This three-wave mixing process can be clearly described by the coupled wave equations (CWE). Under a slowly varying envelope approximation, the CWE of the SHG are expressed as [28]

$$\begin{aligned} \frac{dA_\omega}{dz} &= \frac{2id_{eff}{\omega_1}^2}{k_1c^2}A_{2\omega}A_\omega^* e^{-i\Delta kz} \\ \frac{dA_{2\omega}}{dz} &= \frac{id_{eff}{\omega_2}^2}{k_2c^2}A_\omega^2 e^{i\Delta kz} \end{aligned}, \tag{1}$$

where A_ω and $A_{2\omega}$ are the complex envelopes of the pump and SH waves, respectively, z is the propagation axis, d_{eff} is the effective coefficient of the nonlinear susceptibility tensor which

Optics EXPRESS

is determined by the selected polarization transformation in the SHG. Here, the pump wave polarization is selected as the y-direction parallel to the + c axis of the $LiNbO_3$ crystal; d_{eff} is selected as d_{33} for the conversion of $e_\omega + e_\omega \rightarrow e_{2\omega}$, where e denotes the extraordinary wave; $k_1 = n(\omega) \cdot \omega/c$ and $k_2 = n(2\omega) \cdot 2\omega/c$ are the respective wave vectors, and $\Delta k = 2k_1 - k_2$ is the vector corresponding to the phase mismatch because of material dispersion $n(2\omega) \neq n(\omega)$. To obtain efficient beam output, the phase mismatch must be well compensated. Here, we adopt a method called quasi-phase matching [29] where the nonlinear coefficient d_{eff} is periodically modulated in the propagation direction as shown in Fig. 1; here, $d_{eff} = d_{33} sign\{\cos[(2\pi/\Lambda) \cdot z]\}$. The modulation period is correspondingly determined as $\Lambda = 2\pi/\Delta k$.

The complex amplitude of a pump optical field with arbitrary phase distribution can be expressed as $A_\omega = |A_\omega| \exp[i\varphi_\omega(x, y)]$. Under the above nonlinear coefficient modulation, the complex amplitude of the generated SH optical field can be derived from Eq. (1) under the non-depletion approximation for the pump beam:

$$\begin{aligned} A_{2\omega}(z_0) &= \frac{2id_{33}{\omega_2}^2}{k_2 c^2} |A_\omega|^2 \exp[i2\varphi_\omega(x, y)] \int_0^{z_0} sign\left[\cos\left(\frac{2\pi}{\Lambda} z\right)\right] e^{i\Delta k z} dz \\ &\approx \frac{2id_{33}{\omega_2}^2 f_1 z_0}{k_2 c^2} |A_\omega|^2 \exp[i2\varphi_\omega(x, y)] \end{aligned}, \tag{2}$$

where f_1 is the first Fourier coefficient corresponding to the reciprocal lattice vector $G_1 = 2\pi/\Lambda = \Delta k$. From Eq. (2), it is easy to determine that on undergoing the nonlinear SHG process, the phase of the pump optical field is directly structured as follows:

$$\varphi_{2\omega}(x, y) = 2\varphi_\omega(x, y), \tag{3}$$

3. Topological phase transition of the optical field in SHG

Based on the result of Eq. (3), we further investigate the topological regulation of the optical field accompanied by frequency conversion. The optical field topology is defined with respect to the phase in transverse space. The corresponding topological invariant or topological charge is the number of phase singularities where the phase is undefined [30]. In three-dimensional space, phase singularities manifest themselves as lines of zero intensity. The phase of the optical field increases or decreases continuously, surrounding these lines of zero intensity, with cyclical jumps of 2π. Within a closed path C, the topological invariant t can be calculated by the integral of the phase gradient:

$$t \equiv \frac{1}{2\pi} \oint_C \nabla\varphi(r) dr, \tag{4}$$

Similar to the other topological invariants specified by their respective topologies, this defined topological invariant remains constant under arbitrary continuous phase deformations; hence, in this case, although the spatial distribution of the phase and the position of the phase singularities may vary, the number of phase singularities remains unchanged. For example, the evolution of the optical field in dynamic spatial propagation is consistent with this situation. However, when the optical field interacts with matter, the situation differs to a certain extent. During interaction, vast distortion may be applied to the phase structure, possibly resulting in the topological phase transition of the optical field with the creation or annihilation of new optical singularities.

To illustrate this idea, we selected the phase distribution of the pump optical field based on the theoretical analysis of Eq. (4). It can be easily determined that the loop integral in Eq. (4) is directly related to the rotational symmetry; hence, the calculation of the topological invariant can be considerably simplified when the phase is characterized by the azimuthal angle. Further, in the physical framework, the phase of the optical field always cyclically jumps at 2π and then returns to the origin of the phase loop. This feature may affect the topological phase transition of the

Optics EXPRESS

optical field when the phase is structured by the nonlinear process. Under these considerations, we select the phase distribution expressed as

$$\varphi_\omega(x,y) = \alpha\left[\phi(x,y) - \frac{2\pi m}{M}\right], \tag{5}$$

where α is the azimuth parameter which could be any decimal, $\phi(x,y) = \arctan(y/x)$ is the azimuthal angle, M is the number of phase jumps which could be any positive integer, and m is any integer lesser than M. From Eq. (5), it is easy to determine that the phase of the plane wave can be obtained when $\alpha = 0$. When $M = 1$, the well-designed phase exactly fits the phase distribution of the fractional optical vortex.

We then explore the topological effects during light and nonlinear matter interaction. Substituting Eq. (5) in Eq. (4) and combing with the phase relationship expressed by Eq. (3), the values of the topological invariants of the pump and SH optical fields are derived as

$$\begin{aligned} t_\omega &= M \cdot floor(\alpha/M + 1/2) \\ t_{2\omega} &= M \cdot floor(2\alpha/M + 1/2) \end{aligned}, \tag{6}$$

where $floor(x)$ assumes the largest integer value not greater than x. The evolutions of the topological invariants before and after the SHG process are illustrated in Fig. 2. It's necessary to note that the topological invariant characterizing the optical field topology is corresponding to the number of phase singularities, which is not equivalent to the azimuth parameter [31].

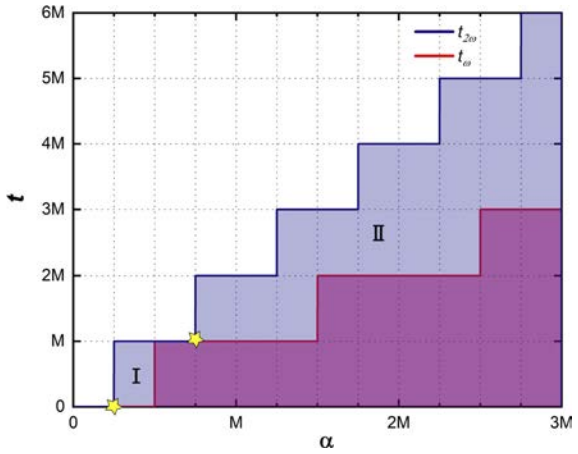

Fig. 2. Diagram of the topological phase transition in SHG. The red and blue lines correspond to the topological invariant values of the pump and SH optical fields, respectively. The critical positions of the topological phase transition are marked by yellow stars. The topological phase transition regions are marked by Roman numerals.

From Fig. 2, the topological phase transition of the optical field governed by the azimuthal parameter α and the number of phase jumps M can be easily determined. It is obvious that there are two critical points (marked by yellow stars) that determine the occurrence of topological phase transition. The values of $\alpha$for these two points are $M/4$ and $3M/4$, respectively. The two intervals (marked by Roman numerals in Fig. 2) in which topological phase transitions occur are specified; when the value of positive $\alpha$is less than $M/4$, or between $M/4$ and $3M/4$, no topological phase transition occurs in the SH optical field. Moreover, the transition steps of the topological invariant are exact integer multiples of the number of phase jumps M; hence, for larger M, a

Optics EXPRESS

potentially steeper topological phase transition will occur in the optical field after nonlinear frequency conversion. It is to be noted that for the case where $\alpha$is negative, the corresponding results are similar to that where it is positive, and only the symbols differ. Therefore, it is not discussed here.

In order to verify the above theory, pump optical fields with different azimuthal parameters are applied, and the results are depicted in Figs. 3 and 4. Figure 3 shows the results of the phase modulation and the accompanying topological phase transition of various fractional optical vortices undergoing the nonlinear SHG process when $M = 1$. The phase singularities are marked by white dotted circles with directional arrows. Intriguingly, the transition of the topological invariant value can be inconsistent with the phase transition; hence, the relationship between the topological invariants before and after the SHG process is not a simple double relationship. For example, the topology of the pumped plane wave does not change after the nonlinear process as shown in Figs. 3(a) and 3(e). The value of the topological invariant of the optical field changes from 3 to 7 instead of 3 to 6 as shown in Figs. 3(m)–3(o). In addition, the phase singularities split when alpha is not an integer which results from the existence of transverse linear momentum.

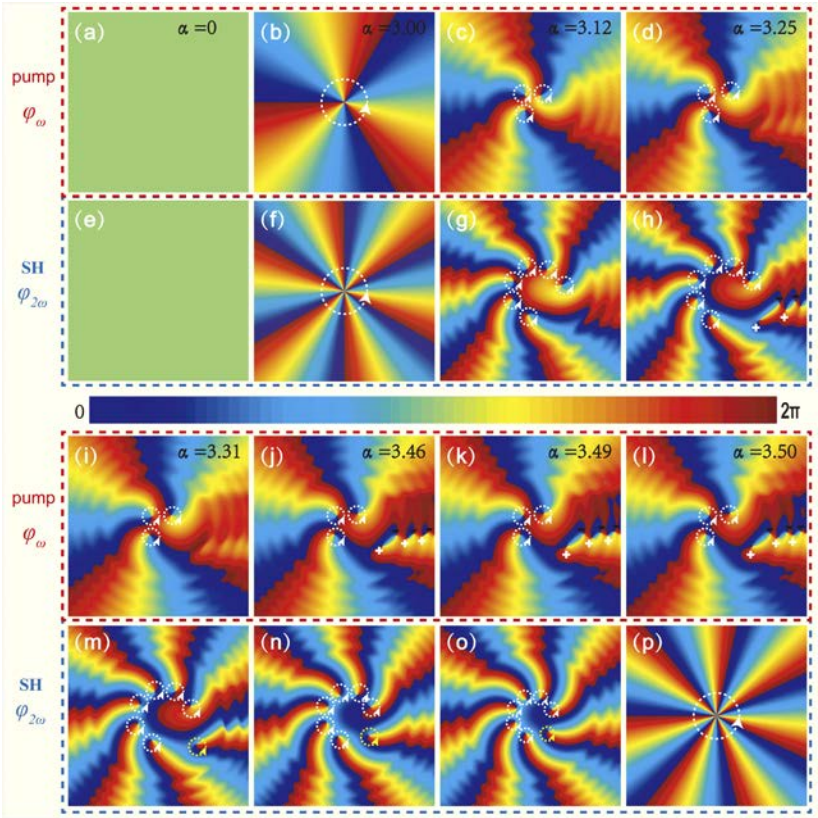

Fig. 3. Topological modulation of the fractional optical vortices in SHG: (a)–(d) and (i)–(l) Phase distributions with various values of α for pump optical fields; (e)–(h) and (m)–(p) Structured phase distributions of the corresponding SH optical fields. The phase singularities are marked by dotted circles with directional arrows.

The impact of phase jumps on the topological phase transition of the optical field is demonstrated in combination with Fig. 4 in which the number of phase jumps is set to seven; the transition steps are considerably greater than that in Fig. 2, and all are exact integer multiples of M. In Figs. 4(a) and 4(e), topological phase transition does not occur for $\alpha < 1.75$, which is the exact

Optics EXPRESS

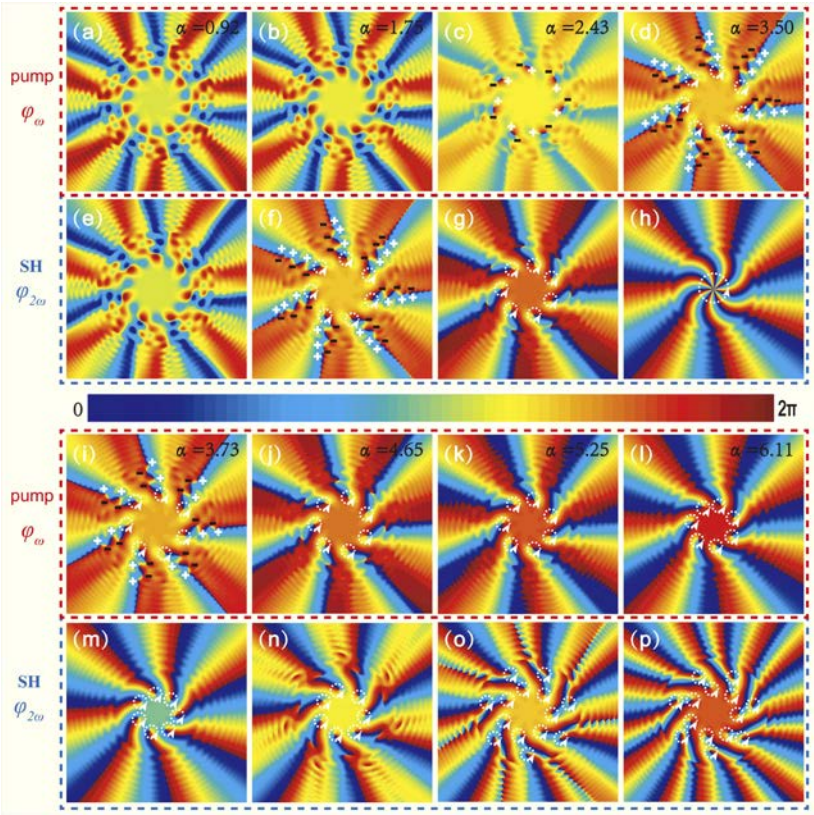

Fig. 4. Optical fields topological modulation for $M = 7$ in SHG: (a)–(d) and (i)–(l) Phase distributions with various values of α for pump optical fields; (e)–(h) and (m)–(p) Structured phase distributions of the corresponding SH optical fields. The phase singularities are marked by dotted circles with directional arrows.

value of $M/4$. However, when $\alpha > 1.75$, seven phase singularities are generated as shown in Figs. 4(c) and 4(g). When $\alpha > 3.50$, the topological phase transition disappears as depicted in Figs. 4(j) and 4(n). For $\alpha > 5.25$, the exact value of $3M/4$, topological phase transition occurs again as shown in Figs. 4(l) and 4(p). In addition, the optical singularity distribution undergoing a topological phase transition can vary in several forms. No extra phase singularities may be generated as shown in Figs. 3(b) and 3(f), or multiple phase singularities may be generated as shown in Figs. 3(m)–3(o) and Fig. 4(g); this depends on whether the OAM of the optical field is intrinsic, as discussed further. In addition, the generation and annihilation of phase singularity pairs marked by white positive and black negative signs, respectively, near the phase transition points are observed as depicted in Figs. 3(j)–3(l) and Fig. 4(c); this indicates that the topological invariant resists continuous perturbations until a topological phase transition occurs [30,32].

4. OAM spectrum analysis

Thus far, we had analyzed the topological phase transition of the optical field during nonlinear frequency conversion mostly from the mathematical point of view, *i.e.*, to examine the evolution of the number of phase singularities before and after the nonlinear process. Further, we consider the essence of this topological effect in detail and explore the corresponding conserved physical

Optics EXPRESS

quantities. In view of the close correlation between the phase singularity and OAM, we first conduct OAM spectrum analysis on the optical field.

An arbitrary optical field $\exp[i\varphi(x,y)]$can be Fourier expanded as $\exp[i\varphi(x,y)] = \sum_l h_l \exp(il\phi)$. For optical fields with the phase defined by Eq. (5), it is a useful mathematical trick to expand it to the form of $\exp[i\varphi(x,y)] = \sum_n h_n \exp[in(M\phi - 2m\pi)]$, and then do some variable substitutions. The Fourier coefficients h_l corresponding to different integer values of OAM l are calculated as

$$h_l = \begin{cases} \frac{M\sin(\alpha\pi/M)}{\pi(\alpha-l)} e^{i\frac{\alpha\pi}{M}} & , \quad l/M \in N \\ 0 & , \quad l/M \notin N \end{cases}, \tag{7}$$

The OAM spectrum$H_l$is generally defined as the result of normalizing $|h_l|^2$. During nonlinear light-matter interaction, the phase structure of the optical field is distorted, and is accompanied by the exchange of energy and linear momentum. Moreover, the OAM spectrum is reshaped due to the coherent superposition of two pump photons carrying the same or different OAM components. The average OAM carried by these optical fields can be obtained from the OAM spectrum, and can be expressed as $L_z' = \sum_l H_l l$. This physical quantity is extrinsic, *i.e.*, dependent on the selection of the rotation axis [33–35], indicating that $L_z'$is sensitive to any subtle continuous disturbance in the optical fields; hence, this is not the physical conserved quantity corresponding to the topological invariant. However, L_z' can be considered as the result of a lateral shift of the rotation axis on the total OAM in the propagation direction L_z, which has been extensively demonstrated as [35]:

$$L_z' = \int [(r - r_0) \times p]_z d\mathrm{x} = L_z - x_0 P_y - y_0 P_x, \tag{8}$$

where $\mathrm{x} = (x, y)$ is the calculated plane, p is the linear momentum density of the optical fields, $r_0 = (x_0, y_0, \mathrm{z})$ is the lateral shift of the prime rotation axis r, and $P_\perp = (P_x, P_y)$ is the total transverse linear momentum. The above equation indicates that $L_z$is intrinsic, and only when the total linear momentum vector points in the z direction, *i.e.*, there is no net lateral linear momentum,L_z is equivalent to L_z'. When the optical field undergoes the nonlinear SHG process, the average OAM L_z' changes with the shaping of the OAM spectrum; whereas, the total OAM in the z direction L_z is unaltered regardless of the variation in the OAM spectrum when no topological phase transition occurs. Only when the light field undergoes a topological phase transition, L_z increases or decreases accordingly. To demonstrate this, the OAM spectra of the optical fields for $M = 7$ before and after frequency conversion are calculated as shown in Fig. 5.

The results depicted in Figs. 5(a) and 5(g) show that there are no topological phase transitions in the pump optical field, as indicated by the yellow solid circles. In this case, the total OAM in the z-direction remains unchanged before and after frequency conversion, although the OAM spectrums for the SH (blue histograms) and pump (red histograms) optical fields vary considerably. This is similar to the previous work [35], indicating that the result of OAM spectrum shaping herein is only a lateral shift of the rotation axis. Figures 5(d) and 5(i) depict the topological phase transition results in the pump optical field, indicated by yellow solid triangles. In this case, the total OAM in the z-direction increases by multiples of M with the topological phase transition, indicating abundant potential for OAM spectrum regulation during light-nonlinear matter interaction. Moreover, the results of the critical transition points where topological phase transition is about to occur are depicted in Figs. 5(b), 5(e), and 5(h), indicated by yellow solid stars. These above analysis demonstrates that the potential topological phase transition of the optical field during nonlinear frequency conversion is actually the result of total OAM transition in the z-direction through OAM spectrum shaping.

Optics EXPRESS

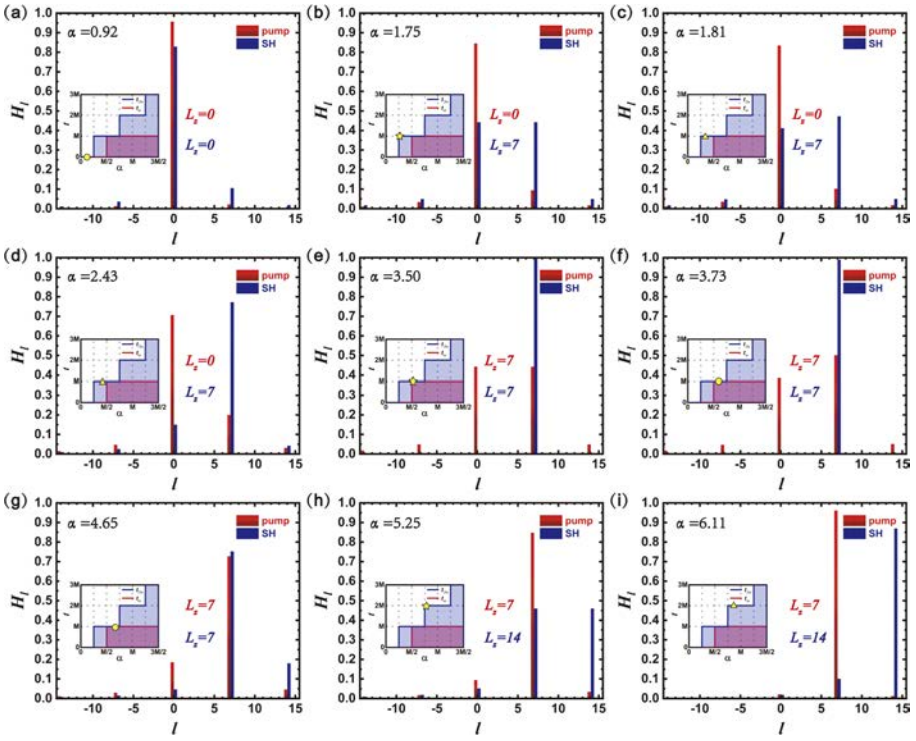

Fig. 5. OAM spectrums of optical fields for $M = 7$ before and after SHG. The red and the blue histograms represent OAM spectrums for pump and SH optical fields, respectively. The potential topological phase transition is indicated with an illustration in each subgraph; the yellow solid circles represent the case for no topological phase transition, the yellow solid stars represent the critical transition points where the topological phase transition just about to happen, and the yellow solid triangles represent the case for topological phase transition.

5. Discussions and conclusions

In early works, several types of structured phase modulation devices [36–38] have been used to realize the topological phase transition of optical fields. The mode transformation and OAM conversion of standard Laguerre-Gaussian modes in SHG have been studied [39,40]. However, the studied optical-field phase was generally structured as a simple helical type $\exp(il\phi)$, with a single phase singularity at the center of the optical axis [41] as shown in Figs. 3(b) and 3(f). The topological phase transition herein, whether through spatial propagation, spin-orbital interaction [42], or nonlinear frequency conversion, is directly characterized by the integer OAM conversion of the central phase singularity without the creation of new phase singularities; hence, the topological invariants of these optical fields can be mapped to the winding number. In this work, we propose that the topology of the optical field can be regulated through frequency control alone, and we study the topological effects during the interaction between more generalized optical fields and nonlinear crystals. The potential topological phase transition is presented and demonstrated. When two-dimensional and three-dimensional nonlinear susceptibility engineered crystals are considered, exotic topological effects may be found; this is intended for future study.

The research system satisfies the law of conservation of energy, linear momentum, and angular momentum. Energy conservation is guaranteed by the frequency conversion relationship $\omega_2 = 2\omega_1$. Nonlinear $LiNbO_3$ crystals imprint the quasi-linear-momentum $G_1 = 2\pi/\Lambda$ on the interacting photons guaranteeing linear momentum conservation. The pump optical field

Optics EXPRESS

can be decomposed into wave components that carry the integer OAM. During the frequency conversion process, the amplitude of these components, as well as the carried OAM, are coherently superimposed on each other; this guarantees the conservation of the angular momentum, resulting in the simultaneous shaping of the OAM spectrum.

In addition, the nonlinear SHG process is mainly studied in this work. When considering higher harmonic frequency conversion, the topological effects may slightly differ, and can be demonstrated accordingly. Larger topological phase transition may be realized by the coherent superposition of more photons, and the critical transition points can be determined as well.

In summary, in this study, we have proposed and demonstrated the topological effects in optical fields during the nonlinear frequency conversion process, and determined the potential topological phase transition. Optical fields with various structured phases were studied in quasi-phase matched SHG using nonlinear coefficient engineered $LiNbO_3$ crystals. The mapping relationship between the phase parameters and the topological invariant was derived, providing two critical transition points associated with the number of phase jumps. Furthermore, we conducted OAM spectrum analysis to reveal the inner mechanism of this topological modulation, and established that the transition of the total OAM in the propagation direction was the physical origin of the topological phase transition. This work provides a new perspective to examine nonlinear light-matter interaction in addition to the traditional degrees of freedom.

Funding

National Key Research and Development Program of China (2017YFA0303700); National Natural Science Foundation of China (11704182, 11604144, 11874214, 61490714).

Disclosures

The authors declare no conflicts of interest.

References

1. H. Rubinsztein-Dunlop, A. Forbes, M. V. Berry, M. R. Dennis, D. L. Andrews, M. Mansuripur, C. Denz, C. Alpmann, P. Banzer, T. Bauer, E. Karimi, L. Marrucci, M. Padgett, M. Ritsch-Marte, N. M. Litchinitser, N. P. Bigelow, C. Rosales-Guzmán, A. Belmonte, J. P. Torres, T. W. Neely, M. Baker, R. Gordon, A. B. Stilgoe, J. Romero, A. G. White, R. Fickler, A. E. Willner, G. Xie, B. McMorran, and A. M. Weiner, "Roadmap on structured light," J. Opt. **19**(1), 013001 (2017).
2. P. Chen, L.-L. Ma, W. Hu, Z.-X. Shen, H. K. Bisoyi, S.-B. Wu, S.-J. Ge, Q. Li, and Y.-Q. Lu, "Chirality invertible superstructure mediated active planar optics," Nat. Commun. **10**(1), 2518 (2019).
3. W. Zhang, J. Tang, P. Chen, G. Cui, Y. Ming, W. Hu, and Y.-Q. Lu, "Evolution of orbital angular momentum in a soft quasi-periodic structure with topological defects," Opt. Express **27**(15), 21667–21676 (2019).
4. Y. Ming, P. Chen, W. Ji, B.-Y. Wei, C.-H. Lee, T.-H. Lin, W. Hu, and Y.-Q. Lu, "Tailoring the photon spin via light–matter interaction in liquid-crystal-based twisting structures," npj Quantum Mater. **2**(1), 6 (2017).
5. V.-C. Su, C. H. Chu, G. Sun, and D. P. Tsai, "Advances in optical metasurfaces: fabrication and applications [Invited]," Opt. Express **26**(10), 13148–13182 (2018).
6. Y. Xu, J. Sun, J. Frantz, M. I. Shalaev, W. Walasik, A. Pandey, J. D. Myers, R. Y. Bekele, A. Tsukernik, J. S. Sanghera, and N. M. Litchinitser, "Reconfiguring structured light beams using nonlinear metasurfaces," Opt. Express **26**(23), 30930–30943 (2018).
7. M. J. Escuti, J. Kim, and M. W. Kudenov, "Controlling light with geometric-phase holograms," Opt. Photonics News **27**(2), 22–29 (2016).
8. E. Cohen, H. Larocque, F. Bouchard, F. Nejadsattari, Y. Gefen, and E. Karimi, "Geometric phase from Aharonov–Bohm to Pancharatnam–Berry and beyond," Nat. Rev. Phys. **1**(7), 437–449 (2019).
9. L. Novotny and N. van Hulst, "Antennas for light," Nat. Photonics **5**(2), 83–90 (2011).
10. N. Yu and F. Capasso, "Flat optics with designer metasurfaces," Nat. Mater. **13**(2), 139–150 (2014).
11. M. Z. Hasan and C. L. Kane, "Colloquium: Topological insulators," Rev. Mod. Phys. **82**(4), 3045–3067 (2010).
12. F. Tang, H. C. Po, A. Vishwanath, and X. Wan, "Comprehensive search for topological materials using symmetry indicators," Nature **566**(7745), 486–489 (2019).
13. L. Lu, J. D. Joannopoulos, and M. Soljačić, "Topological photonics," Nat. Photonics **8**(11), 821–829 (2014).
14. L. Lu, J. D. Joannopoulos, and M. Soljačić, "Topological states in photonic systems," Nat. Phys. **12**(7), 626–629 (2016).

Optics EXPRESS

15. T. Ozawa, H. M. Price, A. Amo, N. Goldman, M. Hafezi, L. Lu, M. C. Rechtsman, D. Schuster, J. Simon, O. Zilberberg, and I. Carusotto, "Topological photonics," Rev. Mod. Phys. **91**(1), 015006 (2019).
16. J. F. Nye, M. V. Berry, and C. Frank Frederick, "Dislocations in wave trains," Proc. R. Soc. Lond. A **336**(1605), 165–190 (1974).
17. M. Yamada, N. Nada, M. Saitoh, and K. Watanabe, "First-order quasi-phase matched LiNbO3waveguide periodically poled by applying an external field for efficient blue second-harmonic generation," Appl. Phys. Lett. **62**(5), 435–436 (1993).
18. S. Trajtenebrg-Mills and A. Arie, "Shaping light beams in nonlinear processes using structured light and patterned crystals," Opt. Mater. Express **7**(8), 2928–2942 (2017).
19. M.-Y. Wang, J. Tang, H.-J. Wang, Y. Ming, Y. Zhang, G.-X. Cui, and Y.-Q. Lu, "Generation of second-harmonic Ince-Gaussian beams," Appl. Phys. Lett. **113**(8), 081105 (2018).
20. Y. Ming, J. Tang, Z.-X. Chen, F. Xu, L.-J. Zhang, and Y.-Q. Lu, "Generation of N00N state with orbital angular momentum in a twisted nonlinear photonic crystal," IEEE J. Sel. Top. Quantum Electron. **21**(3), 225–230 (2015).
21. D. Wei, C. Wang, H. Wang, X. Hu, D. Wei, X. Fang, Y. Zhang, D. Wu, Y. Hu, J. Li, S. Zhu, and M. Xiao, "Experimental demonstration of a three-dimensional lithium niobate nonlinear photonic crystal," Nat. Photonics **12**(10), 596–600 (2018).
22. T. Xu, K. Switkowski, X. Chen, S. Liu, K. Koynov, H. Yu, H. Zhang, J. Wang, Y. Sheng, and W. Krolikowski, "Three-dimensional nonlinear photonic crystal in ferroelectric barium calcium titanate," Nat. Photonics **12**(10), 591–595 (2018).
23. W. H. Lee, "Binary computer-generated holograms," Appl. Opt. **18**(21), 3661–3669 (1979).
24. X.-H. Hong, B. Yang, C. Zhang, Y.-Q. Qin, and Y.-Y. Zhu, "Nonlinear volume holography for wave-front engineering," Phys. Rev. Lett. **113**(16), 163902 (2014).
25. T. Ellenbogen, N. Voloch-Bloch, A. Ganany-Padowicz, and A. Arie, "Nonlinear generation and manipulation of Airy beams," Nat. Photonics **3**(7), 395–398 (2009).
26. B. Yang, X.-H. Hong, R.-E. Lu, Y.-Y. Yue, C. Zhang, Y.-Q. Qin, and Y.-Y. Zhu, "2D wave-front shaping in optical superlattices using nonlinear volume holography," Opt. Lett. **41**(13), 2927–2929 (2016).
27. A. Karnieli and A. Arie, "All-optical Stern-Gerlach effect," Phys. Rev. Lett. **120**(5), 053901 (2018).
28. R. W. Boyd, *Nonlinear optics* (Academic, 2008).
29. J. A. Armstrong, N. Bloembergen, J. Ducuing, and P. S. Pershan, "Interactions between light waves in a nonlinear dielectric," Phys. Rev. **127**(6), 1918–1939 (1962).
30. G. J. Gbur, *Singular optics* (Crc, 2016).
31. J. Zhu, P. Zhang, D. Fu, D. Chen, R. Liu, Y. Zhou, H. Gao, and F. Li, "Probing the fractional topological charge of a vortex light beam by using dynamic angular double slits," Photonics Res. **4**(5), 187–190 (2016).
32. G. Gbur, "Fractional vortex Hilbert's hotel," Optica **3**(3), 222–225 (2016).
33. A. T. O'Neil, I. MacVicar, L. Allen, and M. J. Padgett, "Intrinsic and extrinsic nature of the orbital angular momentum of a light beam," Phys. Rev. Lett. **88**(5), 053601 (2002).
34. S. N. Alperin and M. E. Siemens, "Angular momentum of topologically structured darkness," Phys. Rev. Lett. **119**(20), 203902 (2017).
35. R. Zambrini and S. M. Barnett, "Quasi-intrinsic angular momentum and the measurement of its spectrum," Phys. Rev. Lett. **96**(11), 113901 (2006).
36. P. Genevet, N. Yu, F. Aieta, J. Lin, M. A. Kats, R. Blanchard, M. O. Scully, Z. Gaburro, and F. Capasso, "Ultra-thin plasmonic optical vortex plate based on phase discontinuities," Appl. Phys. Lett. **100**(1), 013101 (2012).
37. N. R. Heckenberg, R. McDuff, C. P. Smith, and A. G. White, "Generation of optical phase singularities by computer-generated holograms," Opt. Lett. **17**(3), 221–223 (1992).
38. N. V. Bloch, K. Shemer, A. Shapira, R. Shiloh, I. Juwiler, and A. Arie, "Twisting light by nonlinear photonic crystals," Phys. Rev. Lett. **108**(23), 233902 (2012).
39. K. Dholakia, N. B. Simpson, and M. J. Padgett, "Second-harmonic generation and the orbital angular momentum of light," Phys. Rev. A **54**(5), R3742–R3745 (1996).
40. J. Courtial, K. Dholakia, L. Allen, and M. J. Padgett, "Second-harmonic generation and the conservation of orbital angular momentum with high-order Laguerre-Gaussian modes," Phys. Rev. A **56**(5), 4193–4196 (1997).
41. L. Allen, M. W. Beijersbergen, R. J. C. Spreeuw, and J. P. Woerdman, "Orbital angular momentum of light and the transformation of Laguerre-Gaussian laser modes," Phys. Rev. A **45**(11), 8185–8189 (1992).
42. L. Marrucci, C. Manzo, and D. Paparo, "Optical spin-to-orbital angular momentum conversion in inhomogeneous anisotropic media," Phys. Rev. Lett. **96**(16), 163905 (2006).